


Analysis of Secondary Refining Slag Parameters with Focus on Inclusion Cleanliness

Julio Anibal Morales Pereira^{a*}, Vinicius Cardoso da Rocha^a, Ayumi Yoshioka^b,

Wagner Viana Bielefeld^a, Antônio Cezar Faria Vilela^a

^aDepartamento de Metalurgia, Universidade Federal do Rio Grande do Sul, Porto Alegre, RS, Brasil

^bDepartamento de Pesquisa e Desenvolvimento, Gerdau Charqueadas, Charqueadas, RS, Brasil

Received: April 23, 2018; Accepted: June 26, 2018

Secondary refining slag samples with different chemical compositions (45-54 % CaO, 7-13 % Al₂O₃, 20-29 % SiO₂, 9-16 % MgO, 0-5 % CaF₂) were investigated to verify the influence of their effective viscosity on inclusion cleanliness of DIN 38MnS6 in a steelmaking plant. The steel samples were collected during the production process for analysis of inclusions. Using the commercial software FactSage 6.4, thermodynamic calculations were performed to determine the effective viscosity, solid fraction, liquid fraction and MgO saturation point of these slags at 1560°C. The results showed that all the slags were saturated in MgO, revealing a better protection of the ladle refractory. The addition of 2 to 5 % of CaF₂ reduced the effective viscosity values for the analyzed slags from 0.45 Pa·s to 0.10 Pa·s, in comparison to the slags without the addition of CaF₂, with an effective viscosity of 0.40 Pa·s, 0.27 Pa·s and 0.22 Pa·s, decreasing the level of non-metallic inclusions for some of the analysed heats. However, it was detected during the manufacturing process that high slag fluidity and re-oxidation events continue to be a challenge associated with reducing the level of non-metallic inclusions.

Keywords: *refining slags, viscosity, inclusions, clean steels, secondary metallurgy.*

1. Introduction

The DIN 38MnS6 steel, due to its application in the mechanical industry through automotive components, requires that steel-melting shops improve the conditions for clean steel production (reduction of inclusions) during the manufacturing process. Through these improved conditions, the mechanical properties and, especially, fatigue of this type of steel are guaranteed, increasing the quality of steel produced by the industry. Conditions which can be improved in this context, are those of the secondary steel refining processes, where the chemical composition and effective viscosity of the slag used has a significant effect on the kinetics of the refining reactions. Furthermore, these conditions add to the removal and dissolution of inclusions throughout the steel-slag interface, as well as facilitate the removal of gases from liquid steel¹⁻⁹. In order to achieve these conditions, metallurgists often prefer completely liquid slags in the ladle treatment. Slags with high solid phase fractions can increase their viscosity and delay refining operations. Since changing the slag composition has a strong effect on its viscosity, it is common to use slags containing fluorite (CaF₂), as this reduces their viscosity and melting point. The addition of alumina (Al₂O₃) should amplify this effect and produce slags with higher liquid fraction^{3,10-15}. The impact of top slag viscosity has been investigated by many researchers. Sui et al.³ indicate that additions of CaF₂ and Al₂O₃ in the slag used in the refining unit effectively decrease the slag viscosity. Wu¹², concludes that the effect of CaF₂ on viscosity

strongly depends on the composition of the slag, and this effect is greater on slags with higher SiO₂ content. For high basicity slags, CaF₂ represses the precipitation of solid phases at low temperatures, leading to low viscosities compared to slags without the presence of CaF₂. Shahbazian et al.¹⁶, reports that in liquid slags containing Al₂O₃, aluminate complexes Al₃O₇⁵⁻, AlO₂⁻, AlO₃³⁻ can be formed. As the amount of CaF₂ increases, aluminate anions can be depolymerized. The disintegration of the aluminate complexes into smaller units results in a decrease in viscosity. According to the studies of Asth¹⁴ and Bartosiaki et al.^{17,18}, an excess of refractory oxides (CaO and MgO) can increase the viscosity of slags due to the presence of solids (CaO precipitation or CaO rich phases, spinels (MgO·Al₂O₃) and MgO) which are detrimental to the process of nonmetallic inclusion removal. According to Valdez et al.⁷, increasing the viscosity of the slag (by the effect of solid phase precipitation) causes a much longer time for the inclusions to be completely removed from liquid steel, and in the case of a low viscosity slag, the particle can be more easily removed through it. Studies of the influence of basicity on the viscosity of the refining slag have concluded that with higher basicity the slag shows less viscous behavior at the same temperature¹⁹⁻²¹. According to Monaghan and Chen¹, in addition to the change in slag viscosity, the dissolution rate of spinel inclusions increases with increasing slag basicity. Kumar and Sankaranarayanan²², Mills^{23,24} and Chuan et al²⁵, apply the concept of optical basicity (Λ) to the viscosity variation of liquid slags (molten silicates), concluding that the introduction of basic oxides (CaO, MgO) disrupt the lattice structure of silicates, resulting in decreased viscosity.

*e-mail: juliolasid@yahoo.com.br

Jönsson et al.¹⁵ verified that for slags of the Al_2O_3 -CaO-MgO-SiO₂ system containing the same contents of 10 % MgO and 10 % SiO₂, from different % Al_2O_3 /% CaO ratios, the increase in CaO content increases the viscosity, with this effect being more significant at temperatures below 1577°C. Xu et al.²⁶, using high-alumina and low SiO₂ slag compositions, similar to those of ladle furnace and ESR slags, study the influence of the %CaO/% Al_2O_3 mass ratio on the viscosity of the slag. The authors concluded that the viscosity decreases with the increase of the %CaO/% Al_2O_3 mass ratio, however, at a determined ratio of %CaO/% Al_2O_3 , the viscosity starts to increase their value. This increase in the viscosity is associated with changes in phases and structures in the slags. Yoon et al.⁵ determined the optimized ratio (%CaO/% Al_2O_3) for bearing steels in the slag between 1.7 and 1.8 by the addition of Al_2O_3 and reduction of the CaO, changing the slag to the composition of slags found in a region of low melting temperature. Dong et al.²⁷ reports that a %CaO/% Al_2O_3 > 2 ratio in slag increases total oxygen, decreasing the ability of slag to absorb oxide inclusions and facilitating high melt temperature inclusions in high ratios.

The objective of this study is to investigate the effects of composition variation of secondary refining slags (with or without CaF₂) by analysing the effective viscosity and the control of non-metallic inclusions as a function of the Al_2O_3 content during the manufacturing process of DIN 38MnS6 steel. As specific objectives, data on steel and slag samples were collected in different stages of a steelmaking plant. In addition, characterization of the non-metallic inclusions in the steel samples and thermodynamic calculations to determine the effective viscosity, solid fraction, liquid fraction and MgO saturation point of these slags were performed in this study. Finally, the different sample types and results are compared and the interactions between slag and inclusions is discussed.

2. Materials and Methods

Industrial sampling method, chemical analysis, thermodynamic calculations, optical basicity calculation and inclusionary analysis will be presented in the following sections.

2.1 Industrial sampling

The DIN 38MnS6 steel, with chemical composition according to the standard²⁸ shown in Table 1, follows these production stages: electric arc furnace (EAF), ladle furnace (LF), vacuum degassing (VD) and solidification in a continuous casting (CC) machine with three strands.

The deoxidation process applied includes aluminum (Al) addition during steel tapping and in the end of the vacuum degassing (VD). The inclusions treatment was provided by addition wire CaSi. Steel and slag samples were collected immediately after the end of the vacuum degassing (VD). Furthermore, steel samples were also taken during the middle of the CC process, at the tundish (sample DT). The middle of the CC process is considered to be when approximately 50 % of steel remains in the ladle, equivalent 30 t.

A total of nineteen heats were evaluated, and the steel samples (AP) were collected with commercial lollipop samplers from Heraeus Electro Nite. The slag samples (EP) were removed by insertion of a steel rod into the slag by the vacuum degassing operator. For the inclusionary analysis, the samples (DT) were collected with samplers without deoxidizer using the Samp-O-Line model, from Heraeus Electro Nite.

2.2 Chemical analysis

Except for the content of [Mg] in steel, all the other elements in the steel were analysed. The steel (AP and DT) and slag samples (EP) were subjected to X-ray fluorescence chemical analysis (FRX) using the equipment from Philips, PW2600 model.

2.3 Thermodynamic calculations

The thermodynamic calculations were performed with the objective of determining the following properties of the slag: solid fraction, liquid fraction, effective viscosity and MgO saturation point at a temperature of 1560°C. The temperature of 1560°C was chosen based on the slag temperature in the continuous casting process. For the thermodynamic calculations, the FactSage 6.4 program was used. The databases applied were FactPS (for pure substances) and FToxid (for oxides and sulfur). As input data, the standard compositions of the A and B slags obtained in fluorescence analysis were applied. The FeO and MnO contents were very low (less than 2.5 wt %) and therefore were disregarded. In the Equilib module, the slag parameters (solid fraction, liquid fraction and MgO saturation point) were determined for a range of MgO content from 0 to 35 wt %, with 1 wt % increments. Through the Viscosity module, the viscosity values of the liquid slag were determined. Finally, the effective viscosity (η_e) was calculated using the Roscoe-Einstein model (Equation 1), which takes into account the solid fraction present in the slag^{3,4,6,13,29}

$$\eta_e = \eta_0(1 - af)^{-n} \quad (1)$$

Table 1. Chemical composition range of DIN 38MnS6 steel studied (% wt).²⁸

Range	C	Si	Mn	Al	P	S	Cr	Mo	Ni	Cu
Mín.	0.36	0.20	1.30	0.010	-	0.045	0.10	-	-	-
Máx.	0.40	0.65	1.60	0.050	0.035	0.065	0.20	0.07	0.25	0.25

where: η_0 = viscosity of liquid slag; f = fraction of precipitated solid phases; a and n are empirical parameters, which are equal to 1.0 and 2.5, respectively, for rigid spherical particles of different sizes and uniformly dispersed.

The FactSage software gives an adequate result for the viscosity calculations with fluoride slags CaO-SiO₂-Al₂O₃-MgO-CaF₂. The FactSage model has been validated in previous studies³⁰⁻³², showing that the difference between calculated and experimental viscosity are estimated to be about 30 %. In fact, the FactSage method has the least amount of errors, when compared to others models.

2.4 Optical basicity (Λ) calculation

The concept of optical basicity has been reported²³ as an alternative to providing measurements of the degree of depolymerization of liquid slags (molten silicates). Optical basicity is determined from the addition of other oxide species, which affect the slag structure and consequently its physical and chemical properties.

Values for viscosity of liquid slag were related to the optical basicity (Λ), determined using Equation 2^{14,22}

$$\Lambda = \sum X_i \cdot \Lambda_i \quad (2)$$

where: $X_i = (x_i \cdot O / \sum x_i \cdot O)$, molar fraction of equivalent cations (molar fraction of each component (x_i) multiplied by the number of moles of oxygen (O) present in the empirical formulas); (Λ_i), optical basicity of the components.

Table 2 shows the optical basicity values of the components used in the calculations. Mills²³ and Pretorius¹⁰ have reported a value of 0.43 and 0.67 for the CaF₂ optical basicity. According to Mills and Shidhar²⁴ this value is very low since the CaF₂ is considered a network breaker, suggesting the value of 1.2. In this study, no significant differences were observed in the calculation of optical basicity between the values 0.67 and 1.2 adopted.

2.5 Inclusionary analysis

The steel samples (obtained with non-deoxidizing samplers) were previously sanded and polished, as recommended by ASTM E3³³, and analysed by ASPEX (Explorer model) equipped with an automated scanning electron microscope (SEM) coupled with an EDS probe, obtaining the chemical composition, shape and diameter of non-metallic inclusions. The pre-set adjustment parameters for automated quantitative analysis were based on ASTM 2142-08²⁹: beam energy of 20.0 kV; 16 ~ 18 mm focus and particle diameter above 4 μ m. The mean surface area of the steel samples examined was 67 \pm 6 mm² for A slags 77 \pm 8 mm² for B slags. In the

Table 2. Optical basicity values for pure oxides and compounds CaF₂ and MgF₂.^{10,23,24}

MgO	SiO ₂	CaO	Al ₂ O ₃	CaF ₂	MgF ₂
0.78	0.48	1	0.61	0.67 (1.2)	0.67

ASPEX analysis, some filters were applied. Table 3 shows the classification rules used by ASPEX in the study of the inclusions of interest, which examine a range of compositions to represent each type of inclusion. In the Table 3, it is important to note that within the classification for *oxides*, the C-A-S (calcium aluminosilicates) type inclusions are also considered.

3. Results and Discussion

3.1 Analysis of the chemical composition and properties of refining slags

The results of the slag chemical compositions and main slag parameters calculated by FactSage 6.4 are shown in Table 4.

As shown in Table 4, two groups of slag are distinguished: A slags, denominated conventional samples, where the contents range from 7-13 % Al₂O₃ and 0-5 % CaF₂ and B slags, denominated adjusted samples, which are of reduced contents and vary between 7-9 % Al₂O₃ and 0-4 % CaF₂.

In Table 4 are the results of the main slag parameters calculated by FactSage 6.4 at the temperature of 1560°C, where the slag viscosity refers to the slag as sampled and where the solid fraction, liquid fraction and effective viscosity correspond to slag at the beginning of the MgO saturation point. The solid phases precipitated and predicted by FactSage 6.4 for all analysed samples, are composed of

Table 3. ASPEX classification rules adopted in this study in the inclusionary analysis.

Types of inclusions	Classification rules
Al-Mg-Ca	Al \geq 30 and Ca \geq 10 and Mg \geq 5 and (Al+Ca+Mg) \geq 70 and (100*S/(Ca+Al+S)) $<$ 10
Al-Mg	Al \geq 50 and Mg \geq 2.5 and (Al+Mg) \geq 70 and (100*S/(Ca+Al+S)) $<$ 10
Alumina	Al \geq 85
Al/Ca 0.8 - 1.5	(Al+Mg+Ca) \geq 5 and (100*S/(Ca+Al+S)) $<$ 10 and Ca $>$ 20 and Al $>$ 20 and (Ca+Al) \geq 65 and Al/Ca \geq 0.8 and Al/Ca $<$ 1.5
Al/Ca 1.5 - 3	(Al+Mg+Ca) \geq 5 and (100*S/(Ca+Al+S)) $<$ 10 and Ca $>$ 20 and Al $>$ 20 and (Ca+Al) \geq 65 and Al/Ca \geq 1.5 and Al/Ca $<$ 3
Al/Ca ovr 3	(Al+Mg+Ca) \geq 5 and (100*S/(Ca+Al+S)) $<$ 10 and Ca $>$ 20 and Al $>$ 20 and (Ca+Al) \geq 65 and Al/Ca \geq 3
Oxides	(Al+Mg+Ca) \geq 5 and (100*S/(Ca+Al+S)) $<$ 10
CaS - Oxide	(Al+Mg) \geq 5 and (Ca+S) \geq 5 and Ca $>$ S and Mn $<$ 5 and Si $<$ 5
CaS-MnS	S \geq 10 and Ca \geq 5 and (Al+Mg) $<$ 5 and Si $<$ 5 and Mn \geq 5
CaS	(Mn+Al+Mg) $<$ 5 and Ca \geq 10 and S \geq 10 and Si $<$ 5

Table 4. Normalized chemical compositions of the investigated slags and main parameters of the slags calculated by FactSage 6.4 at 1560 ° C. (EP samples).

Sequencing	Slag	%CaO	%SiO ₂	%Al ₂ O ₃	%MgO	%CaF ₂	%FeO + ⁹ %MnO	B ₂	CaO/ Al ₂ O ₃	Optical Basicity (Λ)	Solid Fraction	Liquid Fraction	Liquid slag viscosity (Pa.s)	Effective slag viscosity (Pa.s)	MgO Saturation Point(%MgO)
1	A1	50.48	26.83	7.53	12.13	3.03	1.15	1.88	6.7	0.73	0.3	0.7	0.09	0.22	6.21
2	A2	49.36	27.9	10.27	11.96	0.51	1	1.77	4.8	0.72	0.29	0.71	0.11	0.26	7.56
3	A3	50.13	25.63	8.86	11.38	4	1.18	1.96	5.6	0.73	0.17	0.83	0.09	0.14	6.38
4	A4	46.75	28.45	7.12	14.37	3.32	2.33	1.64	6.6	0.72	0.16	0.84	0.10	0.15	10
4	A5	50.69	23.02	10.09	11.13	5.07	1.15	2.2	5.0	0.74	0.07	0.93	0.08	0.1	5.88
4	A6	48.2	25.38	10.26	13.25	2.91	1.08	1.9	4.7	0.73	0.14	0.86	0.09	0.14	7.75
4	A7	49.93	21.75	11.69	13.06	3.57	2.49	2.3	4.3	0.74	0.11	0.89	0.09	0.11	5.59
4	A8	53.08	20.48	12.97	9.46	4.02	1.44	2.59	4.1	0.75	0.04	0.96	0.08	0.09	4.97
1	A9	49.27	23.96	9.97	12.58	4.21	1.95	2.06	4.9	0.73	0.1	0.9	0.09	0.12	6.26
2	A10	46.9	26.19	11.17	15.74	0	1.46	1.79	4.2	0.72	0.3	0.7	0.11	0.27	7.67
3	A11	45.59	26.59	11.49	16.33	0	1.8	1.72	4.0	0.71	0.23	0.77	0.11	0.22	9.02
1	B1	47.95	24.69	8.74	13.41	4.18	1.03	1.94	5.5	0.73	0.15	0.85	0.09	0.13	7.02
2	B2	48.92	28.08	7.49	12.07	2.4	1.04	1.74	6.5	0.72	0.28	0.72	0.10	0.22	7.88
3	B3	47.61	29.36	7.67	14.01	0	1.36	1.62	6.2	0.71	0.39	0.61	0.12	0.4	8.44
1	B4	49.2	26.84	7.11	11.76	3.99	1.12	1.83	6.9	0.73	0.22	0.78	0.09	0.17	7.15
2	B5	53.25	23.56	9.11	9.06	3.72	1.29	2.26	5.8	0.75	0.23	0.77	0.08	0.15	4.42
3	B6	54.67	24.99	8.15	9.17	1.93	1.1	2.19	6.7	0.75	0.43	0.58	0.08	0.45	3.57
1	B7	50.47	24.37	8.36	11.01	3.84	1.95	2.07	6.0	0.74	0.23	0.77	0.09	0.16	5.47
2	B8	48.14	26.91	7.53	13.49	2.04	1.89	1.79	6.4	0.72	0.33	0.67	0.10	0.26	7.19

C_2S (dicalcium silicate) and MgO of similar trend with the results from Rocha et al.²⁹ work.

Based on the results of Table 4, the samples were classified by groups according to the alumina content in the slag, in order to only investigate the influence caused by the different additions of fluorite (CaF_2) on the effective viscosity variation between the two slags series (A and B), shown graphically in Figure 1.

For an Al_2O_3 content of 7-7.5 %, except for the slag sample B3 without CaF_2 , comparison of samples B8, B2, A1, B4 and A4, increasing the additions of CaF_2 between 2-4 % produces a reduction in the effective viscosities of 0.26 Pa·s up to 0.15 Pa·s, with increase of the liquid fractions from 0.67 to 0.84. All samples compared in this category have low binary basicities in the order of 1.6-1.8. The slag sample B8 with addition of 2 % CaF_2 present the value of 0.26 Pa·s of effective viscosity and a liquid fraction of 0.67. The addition of 2.4-3 % CaF_2 in the samples A1 and B2, kept the effective viscosity of the slags to a value of 0.22 Pa·s and the liquid fraction between 0.70 and 0.72 approximately constant. Compared to sample A1, a slight increase of 3.3 % CaF_2 is found in sample A4, which exhibits an effective viscosity fluctuation of 0.15 Pa·s and liquid fraction of 0.84.

For an Al_2O_3 content of 8-8.5%, the samples in the group (B6, B7, A3 and B1), present an effective viscosity change of 0.45 Pa·s to 0.13 Pa·s and a liquid fraction change from 0.58 to 0.85. The samples present binary basicities on the order of 1.94-2.19.

A small tendency towards an increase in the range of effective viscosity and liquid fraction was found in the group (B6, B7, A3 and B1) samples in conjunction with an increase in the CaF_2 content, as compared with the samples with an Al_2O_3 content between 7-7.5 %. Sample B6 with an addition of 2 % CaF_2 , presents an effective viscosity of 0.45 Pa·s. For sample B7 with addition of a slightly lower amount of 3.84 % CaF_2 , it produces an effective viscosity of 0.16 Pa·s. Samples A3 and B1 both with an addition of 4.0 % CaF_2 , reach similar effective viscosities, in the value of 0.14 Pa·s and 0.13 Pa·s respectively.

For an Al_2O_3 content of 9-10%, in samples A2 ($CaF_2 = 0.51$ %), A6 ($CaF_2 = 3$ %), A9 ($CaF_2 = 4.21$), B5 ($CaF_2 \sim 4$ %), A5 ($CaF_2 = 5$ %), the effective viscosities corresponded to the

values of 0.26 to 0.10 Pa·s, with liquid fractions of 0.71 to 0.93, respectively. All samples compared in this category show low binary basicities on the order of 1.8-2.2.

For sample A5, the same tendency as found in the groups above (B6, B7, A3 and B1, as well as B8, B2, A1, B4 and A4) was observed, being a reduction in the effective viscosity and an increase of the liquid fraction with the increase of CaF_2 contents. However, in the case of A5, there was an even higher relation of this tendency compared to the groups mentioned above. Compared with sample A9, the sample B5, exhibits a fluctuation in effective viscosity reduction, possibly due to the insufficient CaF_2 addition with the high 53 % CaO content present in this sample.

For an Al_2O_3 content of 11-13 %, the samples are subdivided into without addition of CaF_2 (0 %), where samples A10 and A11 show an effective viscosity of 0.27 and 0.22 Pa·s, with a liquid fraction of 0.70 and 0.77. And with addition of 4 % CaF_2 , where the samples A7 and A8, reached low effective viscosity in the value of 0.11 Pa·s and 0.10 Pa·s with high liquid fraction of 0.89 and 0.96. All samples compared in this category show binary basicities in the order of 1.7-2.6. Again, slags with the addition of CaF_2 demonstrate the lower effective viscosities and larger liquid fractions in relation to the slags without the addition of CaF_2 .

Moreover, additions of between 2-5 % CaF_2 caused a reduction of the effective viscosities and an increase of the liquid fractions of the slag for the temperature of 1560°C. However, for some of the slag compositions analysed, it has been observed that occasional viscosity fluctuations occur, possibly due to insufficient additions of CaF_2 . In addition, for the same CaF_2 content, with higher Al_2O_3 , the effective viscosity was smaller. These results are consistent with those of other researchers. Wu¹² studied the influence of fluorite addition on high silica slags and its decrease in viscosity, concluding that the effect of CaF_2 on viscosity strongly depends on the composition of the slag, and this effect is greater on slags with high content of SiO_2 than with low SiO_2 content. The presence of CaF_2 should tend to depolymerize the silicate chains or molecules, leading to an expressive decrease in slag viscosity. For slags with high SiO_2 content, CaF_2 reduces the viscosity of the liquid phase and precipitation of the solid phases. For high basicity slags, CaF_2 represses the precipitation of solid phases at low temperatures, leading to low viscosities compared to slags without CaF_2 present. Shahbazian et al.¹⁶, report that in liquid slags containing Al_2O_3 , aluminate complexes $Al_3O_7^{5-}$, AlO_2^- , AlO_3^{3-} can be formed. As the amount of CaF_2 increases, aluminate anions can be depolymerized. The disintegration of the aluminate complexes into smaller units, resulting in a decrease in viscosity.

Regarding the viscosity values predicted by FactSage in this work, they are comparable to the values of viscosity measurements of Wu¹² work, between 0,236-0,079 Pa·s, for compositions of slag between 0-4 % CaF_2 and 25 % Al_2O_3 in

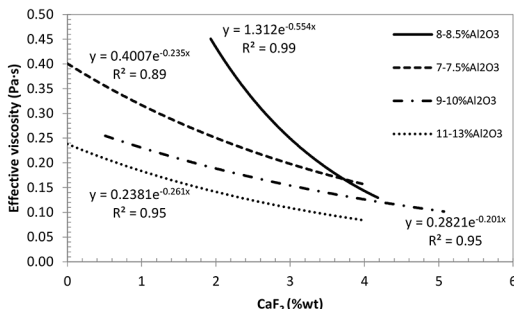


Figure 1. Influence of % CaF_2 additions on the effective viscosity of the slag in different alumina contents

the temperature range of 1424-1632°C. As with the viscosity results of Sui et al.³, less than 1.0 Pa·s for slag compositions of 5 % CaF₂ and 25 % Al₂O₃, in the temperature range of 1400-1500°C were confirmed.

The composition parameters, optical basicity (Λ) and the %CaO/%Al₂O₃ (C/A) ratio of the slags modify effective viscosities and, consequently, their ability in the removal and composition of the inclusions, as can be seen in Figures 2 and 3. The R² of the adjusted data regression for the two relations (Figures 2 and 3), can be considered adequate, given that the data come from the industrial environment, where there are many uncontrolled factors and therefore have been considered as noise.

Figure 2 shows the results of viscosities of liquid slag as a function of the optical basicity values (Λ) for the samples of slags series A and B.

It is observed that the viscosities of liquid slag decrease linearly with an increase of optical basicity (Λ). According to Tang et al.¹⁹ and Pengcheng et al.³⁴, this behavior is associated with the presence of more free oxygen ions (O²⁻) provided by the CaO dissociation when the basicity is increased, destroying the silicate network with a consequent decrease of the slag viscosity. This same trend of results in the influence of optical basicity on viscosity was also obtained by Kumar and Sankaranarayanan²².

Figure 3 shows the influence of the %CaO/%Al₂O₃ ratio on the effective viscosity of the slags.

It is observed that the effective viscosity of the samples of series A vary little with the increase of the %CaO/%Al₂O₃ ratio in relation to the samples of the series B. This behaviour is attributed to series A, because of the higher varying amounts of Al₂O₃ (together with the additions of CaF₂) which maintains the fluidity of the slag with the increase in CaO content. Unlike the B series samples, where an increase in CaO additions with approximately constant Al₂O₃ contents results in a considerable increase in viscosity. Jönsson et al.¹⁵ also verified this tendency for slags of the Al₂O₃-CaO-MgO-SiO₂ system containing the same contents of 10 % MgO and 10 % SiO₂, from different %Al₂O₃/%CaO ratios. The increase in CaO content increases viscosity, with this CaO effect being more significant at temperatures below 1577°C. According to Seok et al.¹³ and Song et al.³⁵, the increase in viscosity is associated with the precipitation of solid particles.

A low viscosity is beneficial for mass transfer in the slag phase, so the choice of such slag composition in the production line should be essential¹⁵. Thus, for both series of slag samples (A and B) it is observed that, to obtain an effective viscosity below 0.20 Pa·s, the optimum range of C/A should comprise 4 < %CaO/%Al₂O₃ < 6.5. This range is much larger than that found by Yoon et al.⁵ for bearing steels, where the ratio (%CaO/%Al₂O₃) optimized in the slag was controlled between 1.7 and 1.8 by the addition of Al₂O₃ and reduction of the CaO, thus changing the composition

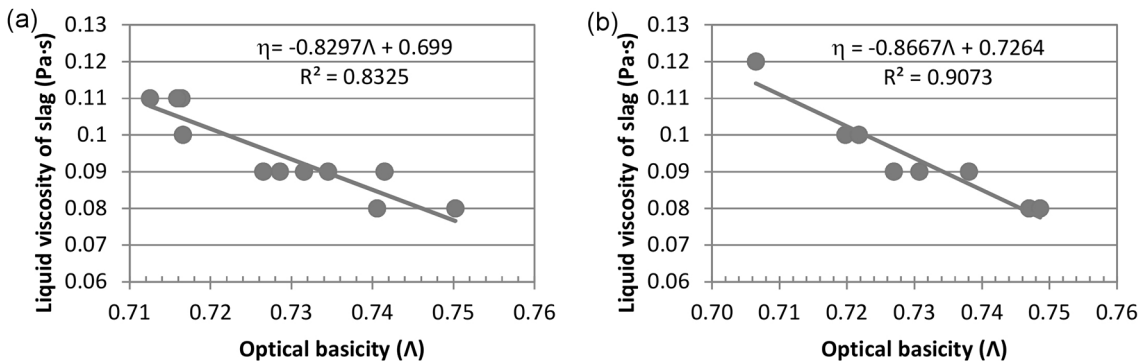


Figure 2. Viscosities of liquid slag versus optical basicity for (a) A slags and (b) B slags

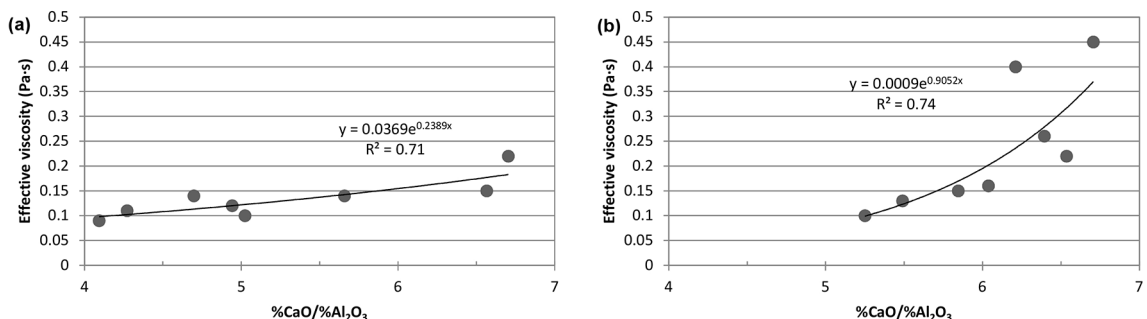


Figure 3. Influence of the % CaO / % Al₂O₃ ratio on the effective viscosity of the slags, being (a) A slags and (b) B slags

of the slag to the region of low melting temperature and reducing total oxygen.

3.2 Inclusionary analysis

Figure 4 shows the typical distributions of the inclusion compositions for samples A4, A8, B3 and B5, shown on the ternary diagrams of the CaO-Al₂O₃-MgO system.

As can be seen, the compositions of the inclusions for sample A4 are quite heterogeneous and are of a larger number than the inclusions in sample A8. This latter sample presented inclusions of alumina and spinel. In the other hand, for both samples B3 and B5 the inclusions are smaller in number. Sample B3 shows the concentrated inclusions of solid aluminate calcium formed and the inclusions are located near the binary axis CaO-Al₂O₃ of the region of low melting point. In sample B5, less concentrated inclusions rich in CaO and MgO are observed.

Figure 5 shows the inclusion density results for the 2.5-5, 5-15 and 15 μm diameter range, corresponding to the A and B steel samples series. These two groups are separated by the dashed line.

In general, most of the steel samples of the A series exhibit inclusion densities of > 0.10 inclusions/ mm^2 , which is verified for the A1 and A9 samples (first of the sequence), the A2 and A10 samples (second of the sequence), A3 e A11 (3rd sequence) and the A4, A5, A6, A7 samples (both of the 4th sequence). In addition, for the B series, samples B1, B4 and B7 (first heat of the sequence), higher inclusion densities were found in relation to samples B2, B3, B5, B6, and B8, of similar densities of 0.10 inclusions/ mm^2 , similar to the A8 sample. On the other hand, only samples A4, A10, B6 and B8 show inclusions in the diameter $\geq 15 \mu\text{m}$. Capurro et al.³⁶ report that inclusions larger than 15 μm may correspond to inclusions of emulsification, refractory particles or re-oxidation inclusions.

The results of effective viscosities of the slags of both series A and B, Table 4, with or without the presence of fluorite (CaF₂), and their influence on the steel cleanliness regarding the densities, size distribution and chemical composition of the inclusions, were also analysed as a part of this study. This analysis focused on steel samples with the lowest inclusion density.

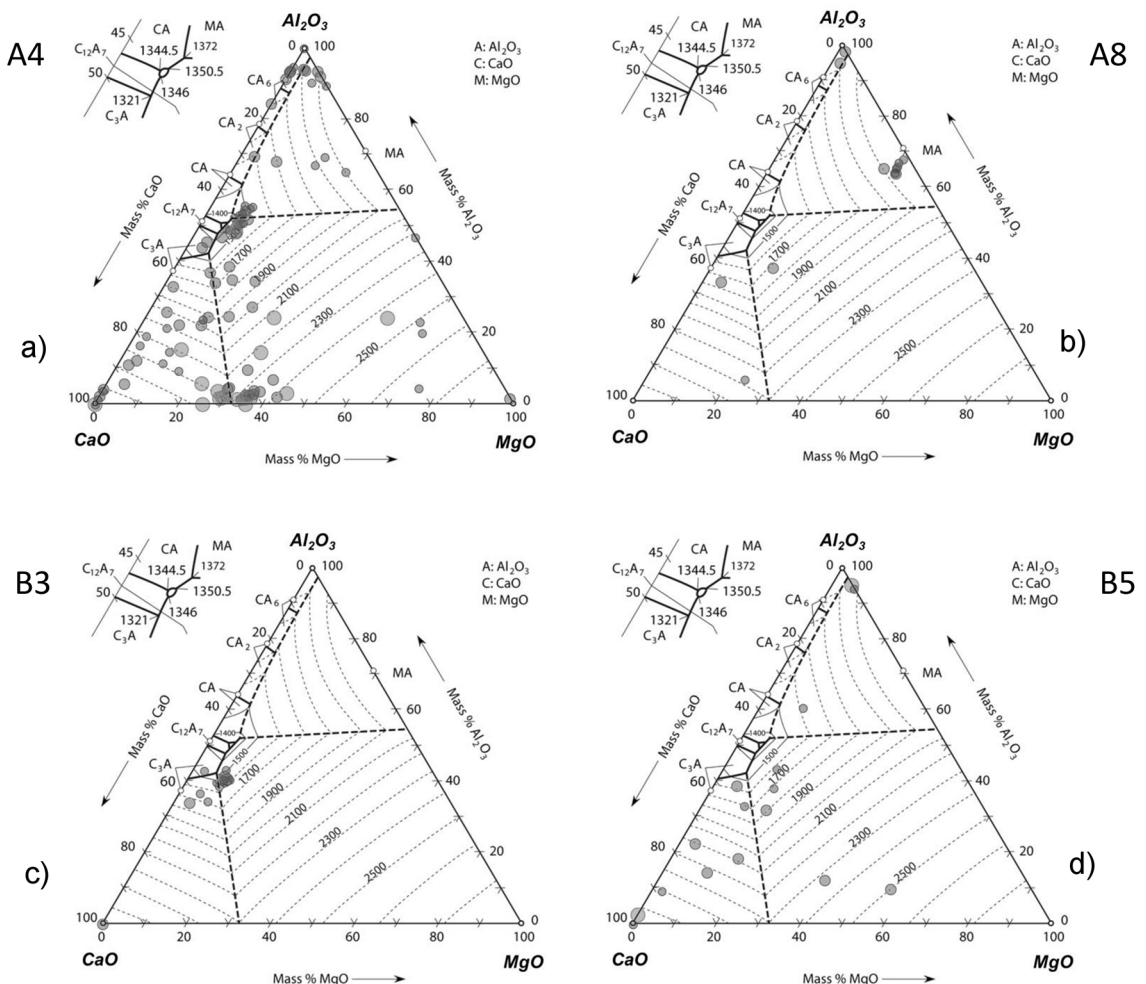


Figure 4. Typical compositions of the oxidized inclusions of the samples: (a) A4, (b) A8 (c). B3, (d) B5. CaO-Al₂O₃-MgO system. Sample DT

As shown in Figure 5, the gradual variation in the population of inclusions in the steel samples with 7-7.5 % Al_2O_3 content, follows the order $\text{A4} > \text{A1} > \text{B4} > (\text{B2} = \text{B3} = \text{B8})$.

The steels samples B2, B3 and B8, present the lowest inclusion densities with 0.10 inclusions/ mm^2 . The B8 steel sample is the only sample of this group with inclusions in the diameter range $\geq 15 \mu\text{m}$. Besides the viscosities and liquid fraction results, the inclusion density, size and composition distribution, give the slag samples B2 ($\text{CaF}_2 = 2.4\%$), and B3 ($\text{CaF}_2 = 0\%$) exceptional conditions for the absorption of inclusions, compared to slag B8. The composition inclusions of sample A4 and B3 are shown in Figure 4.

The variation in the population of inclusions in the steel samples with 8-8.5 % Al_2O_3 content follows the order $\text{B1} > \text{A3} > \text{B7} > \text{B6}$.

The steel sample B6, although it contained the lowest inclusion density, was the only one that presented inclusions in the diameter range $> 15 \mu\text{m}$. This behavior can be explained by the insufficient CaF_2 content ($\text{CaF}_2 = 1.93\%$) added to the CaO solubilization (equivalent to 55 % CaO), which consequently kept a high effective viscosity of 0.45 Pa·s and a smaller liquid fraction of 0.58. Due to the formation of solid compounds, the removal of inclusions in the diameter range $> 15 \mu\text{m}$ was impaired. The CaF_2 content of this slag sample (B6) is the same as slag sample B8 ($\text{CaF}_2 = 2\%$).

In slag samples containing 9-10 % Al_2O_3 , the gradual variation in the population of inclusions of steel samples follows the order $\text{A6} > \text{A5} > \text{A9} > \text{A2} > \text{B5}$. The steel sample B5 presents the lowest inclusion density of 0.10 inclusions/ mm^2 of the samples in the group. The best performance in inclusion removal among the slag sample group was observed in sample B5 and is related to higher CaO content (53 %). However, the distribution of inclusion composition of steel

sample B5 is not concentrated. Slag samples in this group are far from the region of low melting point and close to CaO corner with high content of MgO. The composition inclusions of sample B5 is shown in Figure 4.

In the group of slag samples containing 11-13 % Al_2O_3 , there are no B steel samples for this classification and, the gradual variation in the population of inclusions in the steel samples follows the order $\text{A10} > \text{A7} > \text{A11} > \text{A8}$. Steel sample A8 presents the lowest inclusion density of 0.10 inclusions/ mm^2 . Sample A8, with 4% CaF_2 and containing the highest content of Al_2O_3 (~13 %) in the slag, is attributed with a very low effective viscosity of 0.10 Pa·s and a liquid fraction of 0.96. This slag shows a greater efficiency in the removal of the inclusions due to the low level of density of inclusions obtained. Sui et al.³ indicate that additions of CaF_2 and Al_2O_3 in the slag used in the refining unit in the plant effectively decrease the slag viscosity. Another characteristic of sample A8 is its higher content of 53 % CaO (greater binary basicity - 2,6) among the other slag samples in this category. In addition, although it has the smallest difference between the MgO content in the slag and the saturation start point, it is observed that sample A8, has the largest population of spinel. This can be attributed to a more fluid slag (with a higher liquid fraction) and, therefore, more reactive, contributing to the increase of the spinel inclusions in relation to other samples. See composition inclusions of sample A8 in Figure 4.

From the above, Rocha et al.³⁷ affirms, from experimental results on the inclusion density variation during vacuum degassing, that lower viscosity values are more effective in steel cleanliness. However, higher viscosity values can be harmful to the inclusion removal by slag and an increased

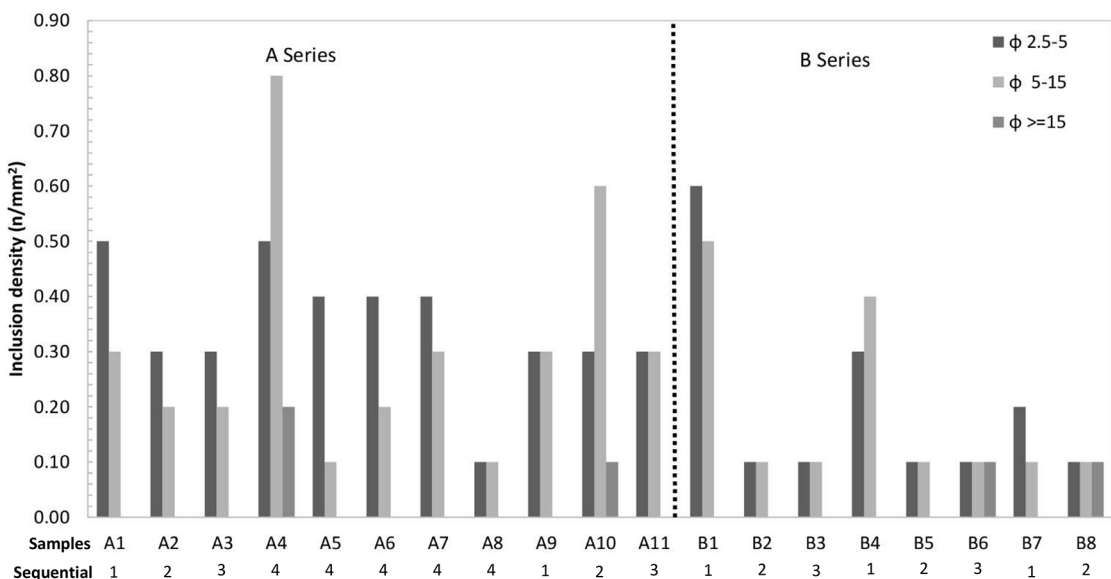


Figure 5. Comparison of density and size distribution of inclusions for A and B steel samples

trend in the inclusion density after vacuum degassing, for all ranges of inclusions.

Another aspect observed in this work is related to the significant influence of the sequence of heats on the discussion of inclusion removal. The samples B1, B4 and B7, Figure 5, present the highest inclusion densities in relation to all other B series steel samples, being verified that they correspond to the first heats of the sequence, which generally suggests that a re-oxidation of these heats occurred during the beginning of the continuous casting. According to Tang and Webler³⁸, it is known from the literature that during the steel transfer operations from the ladle to the tundish, casting of the first heats in the sequence is critical, which can lead to re-oxidation of the steel and consequently an increase in the inclusion density. With respect to the heats of the A series samples, the first heat of the sequence did not present the highest values for inclusion density. Great variation in the inclusion density was observed in another sequence (2nd, 3rd and 4th), however, in these sequences was also shown a hard re-oxidation of steel. The results found in series A did not clarify the effect of the heat sequence on inclusion removal.

When comparing the different types of inclusions found in the steel samples, Figure 6, it was observed that B slags had a better performance in relation to A slags. From the statistical results (frequency of inclusions) it was determined that in relation to the total inclusions, Al_2O_3 inclusions in slag A were (5.1 %) and slag B (3.8 %); for inclusions of $MgO \cdot Al_2O_3$ in slag A (12.3 %) and slag B (1.5 %); $CaO \cdot Al_2O_3 \cdot MgO$ slag A (23 %) and slag B (16 %); $CaO \cdot Al_2O_3$ slag A (7.3 %) and slag B (2.7 %), and CaS inclusions in slag A (2.4 %) and slag B (0.8 %). The inclusions of $CaO \cdot Al_2O_3 \cdot SiO_2$ were the most predominant in both slags, accounting for slag A (50 %) and high values in the slag B (75.4 %).

With respect to the [Al] and [Ca] contents in the steel, the Al content dissolved in the steel is 80 to 140 ppm for slag A and 80 to 90 ppm for slag B. According to Zhao et al³⁹ of their experimental results, Al_2O_3 activity in slag A is higher than in slag B, the [Al] content in liquid steel balanced with slag A is higher than slag B. This fact is confirmed in the present work, where the increase of the Al_2O_3 content in the slag is closely related to the content of [Al]. The contents of [Ca] in steel is 6-11 ppm in slag A, whereas it is 8-9 ppm for slag B. The average %CaO/% Al_2O_3 ratio is slightly higher

for B slag (6.25) than for A slag (5.0), so the CaO supply for the transformation of the inclusions towards the liquid region is favored for slag B^{39,40-42}. In general, it is concluded that Al_2O_3 inclusions are formed as a result of re-oxidation by air (the effect of the oxidation degree in slag is smaller) and the decrease in temperature during the final step of the steel manufacturing process^{9,27,43}. On the other hand, the formation of inclusions of pure spinel ($MgO \cdot Al_2O_3$) is facilitated due to an increase in slag fluidity, which leads to increased MgO erosion of slag line refractories, as well as MgO saturation, which increase the dissolved magnesium in the liquid steel^{1,9,10,17,18,44-48}. Secondary spinel formation by re-oxidation after modification with calcium should also be considered^{38,45,47,49,50}. In addition to these inclusions, formation of inclusions of type CA and CaS exist in a smaller proportion than those of CAS.

Finally, the selection of a specific slag composition to improve the removal of the inclusions, providing adequate viscosity with the lowest number (density), size distribution and inclusion composition, was assigned to the samples A8, B2 and B3. These last two slags had very similar compositions, however, without addition of CaF_2 in sample B3, which indicates a saving process. A possible explanation for this unexpected behavior of sample B3 may be related to other factors than the slag functions, such as stirring of the metal bath, since it is an industrial process and many uncontrolled factors are present, as already pointed out previously²⁹. Future experiments in the laboratory will be carried out to better clarify the effects observed here regarding the cleaning of steel by slag.

4. Conclusions

Analysing industrial data involving steel cleanliness and refining slags is a difficult task due to the various non-controllable factors. However, in this study some important correlations between chemical composition of slag and its ability to remove non-metallic inclusions were established. Through chemical analyses and thermodynamic computational calculations performed for DIN 38MnS6 steel, the following conclusions are presented:

- For the system based on $CaO-SiO_2-Al_2O_3-MgO$, additions of CaF_2 from 2% to 5% and Al_2O_3 from

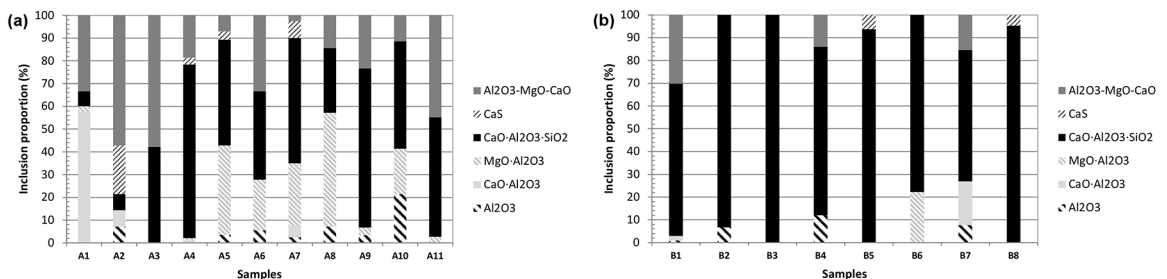


Figure 6. Types of inclusions for steel samples analysed with slag A and B

- 7-13 %, reduced the viscosity of the slag promoting effective viscosities from 0.45Pa·s to 0.10Pa·s;
- For the ranges of slag composition studied, the values of effective viscosities decrease with increasing optical basicity;
- Increase in the %CaO/%Al₂O₃ ratio in the samples of the A slags showed a lower viscosity variation, when compared to the samples of B slags;
- Heats of the first sequencing were more re-oxidized compared with other sequencing positions. Regarding the rest of sequencing, there was no clear distinction;
- Additions of up to 3 % CaF₂, approximately, appear to be insufficient to significantly reduce the viscosity of the slag, making it difficult to remove inclusions of size ≥ 15 μm in heats A4, A10, B6 e B8;
- The increase of MgO in the inclusions was correlated more clearly with the increase of the liquid fraction of the slag. Slag with a minimum of 0.83 of liquid fraction, presented greater amount of spinel inclusions;
- Increase of the liquid fraction of the slag promoted the conditions for the removal of inclusions, however it is important to take into account the negative effect of re-oxidation (generally noted in the first sequencing);
- Comparing A slags with B slags, B slags presented reduction of the alumina content and less re-oxidation events (except in the 1st sequencing), promoting the reduction of alumina and spinel inclusions, as well as the higher formation of CAS-type inclusions, which has an effect in the improvement of steel cleanliness;
- With the objective of an effective removal of the inclusions and reduction of steel-slag-refractory reactions, the optimal recommended viscosity range for the slags studied here was between 0.15-0.22 Pa·s and liquid fractions between 0.70-0.80.

5. Acknowledgements

The authors are grateful to Gerdau Charqueadas, for their collaboration in obtaining the samples and heat data at the plant. Also to the CNPq, for the financial support through the Postdoctoral scholarship (Julio A. M. Pereira).

6. References

1. Monaghan BJ, Chen L. Effect of changing slag composition on spinel inclusion dissolution. *Ironmaking & Steelmaking*. 2006;33(4):323-330.
2. Elfawakhry MK, Fathy A, Eissa M, Mattar T. Effect of steel composition and slag properties on NMI in clean steel production. *MATEC Web of Conferences*. 2016;39:02002.
3. Sui Y, Yue C, Peng B, Wang C, Guo M, Zhang M, et al. Optimization of Slag Chemistry Towards Inclusion Control for 28CrMo47 Drill Pipe Steel Based on Viscosity and Equilibration Studies. *Steel Research International*. 2016;87(6):752-760.
4. Reis BH, Bielefeldt WV, Vilela ACF. Efficiency of Inclusion Absorption by Slags during Secondary Refining of Steel. *ISIJ International*. 2014;54(7):1584-1591.
5. Yoon BH, Heo KH, Kim JS, Sohn HS. Improvement of steel cleanliness by controlling slag composition. *Ironmaking & Steelmaking*. 2002;29(3):214-217.
6. Park JH, Kim DJ. *Interfacial reaction between calcium silicate base flux and high manganese and aluminum alloyed steels*. In: 8th International Conference on Clean Steel; 2012 May 14-16; Budapest, Hungary.
7. Valdez M, Shannon GS, Sridhar S. The Ability of Slags to Absorb Solid Oxide Inclusions. *ISIJ International*. 2006;46(3):450-457.
8. Ma WJ, Bao YP, Wang M, Zhao DW. Influence of slag composition on bearing steel cleanliness. *Ironmaking & Steelmaking*. 2014;41(1):26-30.
9. Valdez M, Prapakorn K, Sridhar S, Cramb AW. *Dissolution of Inclusions in Steelmaking Slags*. In: Proceedings of ISSTech 2003 Conference; 2003 Apr 27-30; Indianapolis, IN, USA. p. 789-798.
10. Pretorius E. *The effect of Fluorspar in Steelmaking Slags*. *Baker Refractories*; 1998. Available from: <<http://etech.lwbref.com/Downloads/Theory/The%20Effect%20of%20Fluorspar%20in%20Steelmaking%20Slags.pdf>>. Access in: 15/5/2018.
11. Gran J, Wang Y, Sichen D. Experimental determination of the liquidus in the high basicity region in the Al₂O₃(30 mass %) - CaO - MgO - SiO₂ system. *Calphad*. 2011;35(2):249-254.
12. Wu L, Gran J, Sichen D. The Effect of Calcium Fluoride on Slag Viscosity. *Metallurgical and Materials Transactions B*. 2011;42:928-931.
13. Seok SH, Jung SM, Lee YS, Min DJ. Viscosity of Highly Basic Slags. *ISIJ International*. 2007;47(8):1090-1096.
14. Asth HG. *Desenvolvimento de escórias de refino secundário para forno panela da V&M do Brasil*. [Dissertation]. Belo Horizonte: Escola de Engenharia da Universidade Federal de Minas Gerais; 2011.
15. Jönsson PG, Jonsson L, Sichen D. Viscosities of LF Slags and Their Impact on Ladle Refining. *ISIJ International*. 1997;37(5):484-491
16. Shahbazian F, Sichen D, Seetharaman S. The Effect of Addition of Al₂O₃ on the Viscosity of CaO-FeO-SiO₂-CaF₂ Slags. *ISIJ International*. 2002;42(2):155-162.
17. Bartosiaki BG, Pereira JAM, Bielefeldt WV, Vilela ACF. *Estudo de inclusões não-metálicas em aços durante tratamento em degaseificador a vácuo e início do lingotamento contínuo*. In: 45º Seminário de Aciaria da ABM; 2014 May 25-28; Porto Alegre, RS, Brazil.
18. Bartosiaki BG. *Caracterização de inclusões não-metálicas de óxidos no aço SAE 52100*. [Graduation Work]. Porto Alegre: Rio Grande do Sul Federal University; 2013.
19. Tang X, Zhang Z, Guo M, Zhang M, Wang X. Viscosities Behavior of CaO-SiO₂-MgO-Al₂O₃ Slag With Low Mass Ratio of CaO to SiO₂, and Wide Range of Al₂O₃ Content. *Journal of Iron and Steel Research, International*. 2011;18(2):1-17.

20. Chang KL, Su YH, Hwang WJ. *Investigation of refining slag properties in production of SM570 welding structural steel*. In: Proceedings of 9th International Conference on Clean Steel; 2015 Sep 8-10; Budapest, Hungary.
21. Gao Y, Wang S, Hong C, Ma X, Yang F. Effects of basicity and MgO content on the viscosity of the SiO₂-CaO-MgO-9wt% Al₂O₃ slag system. *International Journal of Minerals, Metallurgy, and Materials*. 2014;21(4):353-362.
22. Kumar M, Sankaranarayanan SR. Effect of optical basicity on the viscosity of oxide systems. *Journal of Mining and Metallurgy*. 2008;44(1B):133-135.
23. Mills KC. The influence of Structure on the Physico-chemical Properties of Slags. *ISIJ International*. 1993;33(1):148-155.
24. Mills KC, Sridhar S. Viscosities of ironmaking and steelmaking slags. *Ironmaking & Steelmaking*. 1999;26(4):262-268.
25. Hong C, Gao YM, Wang SB. Application of Optical Basicity for Estimation of Viscosity of SiO₂-CaO-MgO-Al₂O₃ System. *Advanced Materials Research*. 2014;1033-1034:811-817.
26. Xu JF, Zeng T, Sheng MQ, Jie C, Wan K, Zhang JY. Viscosity of low silica CaO-5MgO-Al₂O₃-SiO₂ slags. *Ironmaking & Steelmaking*. 2014;41(7):486-492.
27. Dong W, Ni H, Zhang H, Lü Z. Effect of slag composition on the cleanliness of 28MnCr5 gear steel in the refining processes. *International Journal of Minerals, Metallurgy and Materials*. 2016;23(3):269-275.
28. Deutsches Institut für Normung. *DIN EN 10267: ferritic-pearlitic steels for precipitation hardening from hot-working temperatures*. Berlin: Deutsches Institut für Normung; 1998. 20 f.
29. Rocha VC, Pereira J, Yoshioka A, Bielefeldt W, Vilela A. Evaluation of Secondary Steelmaking Slags and Their Relation with Steel Cleanliness. *Metallurgical and Materials Transactions B*. 2017;48(3):1423-1432.
30. Liu Z, Pandelaers L, Jones PT, Blanpain B, Guo M. *Effect of Al₂O₃ and SiO₂ addition on the viscosity of BOF slag*. Advances in Molten Slags, Fluxes, and Salts: Proceedings of the 10th International Conference on Molten Slags, Fluxes and Salts (MOLTEN16); 2016 May 22-25; Seattle, WA, USA. p. 439-445.
31. Rocha VC, Silva ML, Bielefeldt WV, Vilela ACF. Assessment of viscosity calculation for calcium-silicate based slags using computational thermodynamics. *REM Int Eng J*. 2018;71(2):243-252. DOI: <http://dx.doi.org/10.1590/0370-44672017710029>
32. Kim WY, Jung IH, Decterov S, Pelton AD. *Modeling viscosity of molten slags and fluxes*. In: Proceedings of 9th International Conference on Clean Steel; 2015 Sep 8-10; Budapest, Hungary.
33. ASTM International. *ASTM E 3-11 - Standard Guide for Preparation of Metallographic Specimens*. West Conshohocken: ASTM International; 2011.
34. Li P, Ning X. Effects of MgO/Al₂O₃ Ratio and Basicity on the Viscosities of CaO-MgO-SiO₂-Al₂O₃ Slags: Experiments and Modeling. *Metallurgical and Materials Transactions B*. 2016;47(1):446-457.
35. Song M, Shu Q, Sichen D. Viscosities of the Quaternary Al₂O₃-CaO-MgO-SiO₂ Slags. *Steel Research International*. 2011;82(3):260-268.
36. Capurro C, Cerrutti G, Cicutti C. *Influence of vacuum degassing on steel cleanliness*. In: Proceedings of 9th International Conference on Clean Steel; 2015 Sep 8-10; Budapest, Hungary.
37. Rocha VC, Pereira JAM, Yoshioka A, Bielefeldt WV, Vilela ACF. Effective Viscosity of Slag and Kinetic Stirring Parameter Applied in Steel Cleanliness During Vacuum Degassing. *Materials Research*. 2017;20(6):1480-1491.
38. Tan J, Weblar BA. *Reoxidation of inclusions after aluminum deoxidation and calcium treatment*. In: Proceedings of 9th International Conference on Clean Steel; 2015 Sep 8-10; Budapest, Hungary.
39. Zhao S, He SP, Guo YT, Chen GJ, Lv JC. Effect on cleanliness of molten steel with different refining slag systems for low alloy ship plate. *Ironmaking & Steelmaking*. 2016;43(10):790-798.
40. Yang G, Wang X. Inclusion Evolution after Calcium Addition in Low Carbon Al-Killed Steel with Ultra Low Sulfur Content. *ISIJ International*. 2015;55(1):126-133.
41. Deng Z, Zhu M. Evolution Mechanism of Non-metallic Inclusions in Al-Killed Alloyed Steel during Secondary Refining Process. *ISIJ International*. 2013;53(3):450-458.
42. Hu Y, Chen WQ, Han HB, Bai RJ. Influence of calcium treatment on cleanliness and fatigue life of 60Si2MnA spring steel. *Ironmaking & Steelmaking*. 2017;44(1):28-35.
43. Park JH, Todoroki H. Control of MgO·Al₂O₃ Spinel Inclusions in Stainless Steels. *ISIJ International*. 2010;50(10):1333-1346.
44. Tang Y. Effect of Slag Composition on Inclusion Control in LF-VD Process for Ultra-Low Oxygen Alloyed Structural Steel. *Procedia Earth and Planetary Science*. 2011;2:89-97.
45. Capurro C, Cerrutti G, Cicutti C. *Estudio de la generación y modificación de las inclusiones tipo espinelas durante las etapas de metalurgia secundaria y colada continua*. In: Proceedings of 19th IAS Steel Conference; Nov 5-7; 2013. Rosario, SF, Argentina.
46. Okuyama G, Yamaguchi K, Takeuchi S, Sorimachi K. Effect of Slag Composition on the Kinetics of Formation of Al₂O₃-MgO Inclusions in Aluminum Killed Ferritic Stainless Steel. *ISIJ International*. 2000;40(2):121-128.
47. Verma N, Pistorius PC, Fruehan RJ, Potter MS, Oltmann HG, Pretorius EB. Calcium Modification of Spinel Inclusions in Aluminum Killed Steel: Reaction Steps. *Metallurgical and Materials Transactions B*. 2012;43(4):830-840.
48. Jiang M, Wang XH, Wang WJ. Study on refining slags targeting high cleanliness and lower melting temperature inclusions in Al killed steel. *Ironmaking & Steelmaking*. 2012;39(1):20-25.
49. Pretorius EB, Oltmann HG, Cash T. *The effective modification of spinel inclusions by Ca treatment in LCAK steel*. In: Proceedings of AISTech 2009 - Iron and Steel Technology Conference; 2009 May 4-7; St. Louis, MO, USA.
50. Bao S, Wang X, Zhang L, Yang S, Peaslee KD. *Improving Steel Cleanliness Through Slag Refining*. Proceedings of AISTech 2008 - Iron and Steel Technology Conference; 2008 May 5-8; Pittsburgh, PA, USA.